Proceedings of the 8th International Conference on MicroManufacturing
University of Victoria, Victoria, BC, Canada, March 25-28, 2013

Sol-Gel Synthesis of ZrO_2 Coatings on Micro End Mills

ICOMM 2013
No. 35

Justin Morrow[1], M. Isabel Tejedor-Anderson[2], Marc A. Anderson[3,4], Luis A. Ruotolo[5], and Frank E. Pfefferkorn[6•]

[1]Justin Morrow; Mechanical Engr., University of Wisconsin - Madison, USA; e-mail: jdmorrow@wisc.edu
[2] M. Isabel Tejedor-Anderson; Water Sci. and Engr. Lab, UW-Madison, USA; email: mitejedo@wisc.edu
[3]Marc A. Anderson; Water Sci. and Engr. Lab, UW-Madison, USA; email: nanopor@wisc.edu
[4]Marc A. Anderson; Electrochemical Processes Unit, IMDEA Energy Institute, Mostoles (Madrid) SPAIN
[5]Luis A. Ruotolo; Water Sci. and Engr. Lab, UW-Madison, USA; email: ruotolo@wisc.edu
[6]Frank E. Pfefferkorn; Mechanical Engr., UW-Madison, USA; email: pfefferk@engr.wisc.edu•

Key Words: micro end milling, sol-gel, zirconia, dip-coating, electrophoresis

ABSTRACT

The objective of this paper is to develop a coating method for placing ultra-thin zirconia films, fabricated using sol-gel methods, onto micro end mills for purposes of improving performance with respect to tool wear and cutting forces. Sol-gel synthesis is investigated because of its potential as a low energy and inexpensive method for depositing a variety of wear resistant and chemically stable oxide coatings that could potentially reduce forces and extend tool life. Two sol-gel based deposition methods are investigated: dip-coating and electrophoresis. The coatings are deposited on 300-µm-diameter micro end mills, sintered, and tested while cutting 6061-T6 aluminum. Initial results suggest that sol-gel coating methods can produce the required coverage and conformity in the cutting zone. However, preliminary findings show that the coating is removed in the cutting zone after a short time of machining (6 sec). The tool pre-treatment and extent of sintering, which affect surface adhesion require further study and optimization.

INTRODUCTION

Cemented tungsten carbide (WC) with cobalt binder is the most common material used for micro end mills. The high stiffness of WC minimizes tool deflection and can be precision ground. However, WC is also very brittle and excessive force during machining can lead to premature tool fracture. Therefore, many types of coatings for WC tools have been investigated to decrease forces during micro-machining to increase tool life and enable more aggressive cutting conditions for increased productivity. Increasing productivity is of particular importance in micro end milling where the material removal rate is much lower than in macro cutting operations. Previous work has shown that forces can be significantly reduced during micro end milling by applying nanocrystalline diamond coatings, especially for milling in adhesive materials like aluminum [1]. The hardness and low friction coefficient of diamond make it particularly attractive, but diamond is typically not used for machining ferrous alloys due to carbon-iron reactions at elevated temperatures and pressures. Therefore, other hard coatings such as nitrides and oxides have been investigated [2], [3]. Oxide coatings are of interest because they can be deposited at low cost and are typically chemically inert.

Oxide coatings can either be directly synthesized through controlled chemical oxidation of a substrate to obtain a protective surface layer (*e.g.*, Al_2O_3 on aluminum) or by bringing dissimilar metal oxide particles into contact with the substrate and forming a bond at the interface (*e.g.*, ZrO_2 on WC). The latter method is typically used for oxide coatings that are known to have good wear properties (typically alumina or zirconia) and cannot be created directly from typical tool materials (carbide and steel). Oxide coatings are applied through either physical methods such as physical vapor deposition (PVD) and thermal spraying or chemical methods such as chemical vapor deposition and sol-gel synthesis.

PVD involves vaporizing a source material and accelerating the vapor toward the substrate in a vacuum. PVD methods include cathodic arc, electron beam, and unbalanced magnetron sputtering, among others [4]. Thermal spray methods involve using a high velocity gas or plasma to accelerate vaporized oxide particles at the substrate. Commonly used thermal spray methods include high velocity oxy-fuel (HVOF), plasma spray, flame spray, and electric arc spray [5]. The common thread among these methods is that significant kinetic energy is added to the oxide particles in the transport step of deposition and proper bonding is ensured by particle deformation upon impact.

Sol-gel coatings are applied using a chemically derived suspension or *sol* of charge stabilized nanoparticles where the solvent (typically water) provides a natural transport medium for the particles to reach the substrate. The deposition process can proceed in several ways including dip-coating, spin-coating, spray-coating, or electrophoresis [6]. This paper focuses on the dip-coating and electrophoresis deposition methods. In dip-coating, the substrate is dipped into the sol and retracted. The deposition occurs during substrate retraction when capillary forces pull the sol along with the retracting substrate above the sol surface and the suspended

• corresponding author

nanoparticles are left behind as the solvent evaporates [7]. Alternatively, similar sol-gel coatings have been achieved through electro-depostion. This method uses electrophoresis, the motion of charged particles suspended in a viscous medium caused by an applied electric field. Deposition occurs while the electric field is applied and the substrate is in the sol [8].

While both methods (PVD and sol-gel) have been used for depositing oxide coatings on macro-scale cutting tools [3], little research exists in applying oxide coatings to micro-mechanical cutting tools. Coatings for micro end mills produced with the sol-gel process have several advantages over those deposited via PVD:

- Sol-gel synthesis can produce higher purity, conformal coatings by controlling the quality of the parent chemical reagents.
- Sol-gel coatings are deposited at room temperature and pressure.
- Sol-gel coatings can be achieved without outside energy to transport the oxide particles to the tool surface and achieve adhesion. The aqueous suspension provides a natural vehicle for oxide particle transport to the tool surface and allows complex geometries to be coated easily.
- The sol-gel coating process is flexible in the type of coatings that can be produced since the pure zirconia nanoparticles could easily be replaced by alumina or partially stabilized zirconia (PSZ).
- Sol-gel coating is more environmentally friendly because no organic solvents are used and minimal energy input is required. However, some heating may be required (*i.e.*, sintering) to achieve optimal coating properties. The present method uses a radiative surface heating method that requires under 50 W for one hour per sintering cycle.

Many of these advantages of sol-gel coatings were stated by Uhlman and Teowee in a paper surveying the areas of likely growth potential for sol-gel chemistry [9].

This paper will present two synthesis routes (dip-coating and electrophoresis) to obtain ultra-thin (~ 200-nm-thick) pure zirconium oxide (ZrO_2) coatings on micro end mills and evaluate the performance of this coating during machining of 6061-T6 aluminum alloy.

COATING PROCEDURE

A. PREPARATION OF SOL AND TOOLS

Two-flute, 300-µm-diameter (0.0120 in.), end mills (PMT part TS-2-0120-S) are ultrasonically cleaned in methanol and allowed to dry in air after receipt from the manufacturer. The cleaned end mills are then placed in a furnace at 300ºC in air for 2 hours to promote mild oxidation of the tool surface for improved oxide adhesion of the coating. The sol of ZrO_2, with particles of approximately 3-nm-diameter is synthesized by using a hydrolysis/condensation route from zirconium propoxide in acidic media [10]. All reagents used in the synthesis are AC grade and the water Milli-Q. The concentration of ZrO_2 stock sol is 22 g/l. Sols with concentration of 11 g/l and 3 g/l are prepared by diluting the stock sol with an HCl solution of pH 2.3.

Two methods are tested to deposit zirconia coatings using a zirconia ZrO_2 zirconia nanoparticle sol: dip-coating and electrophoresis.

B. DIP-COATING

In the dip-coating method, the pre-treated tools are placed in a holder and fully immersed into the 11g/l concentration sol for 30 seconds, then retracted at a speed of 1.46 mm/s with the cutting tip pointed upwards (*i.e.*, opposite direction of gravity), and allowed to dry in air for 30 minutes. A controlled drying step is then performed in a furnace at 70ºC in air for 1 hour. The coatings are sintered after drying under a vacuum (0.08 Torr) at 900°C for 1 hour. The coating thickness in the dip-coating method is controlled through the sol concentration and the rate of withdrawing the tool from the sol.

C. ELECTROPHORESIS

The electrophoresis method differs from the dip-coating method in that an electric field is applied to the sol to move the charge stabilized nanoparticles toward the tool surface. The electrophoretic cell is constructed by suspending a pre-treated tool (working electrode) by the shank with the cutting tip pointed downwards into a beaker of sol with a ring of titanium (counter-electrode) lining the interior (Fig. 1). A potentiostat is used to apply a constant electrode potential to the working electrode. All potentials are referred to a calomel saturated electrode (SCE). Considering the particles are positively charged, the tool is cathodically polarized at – 0.5 or -1.0 V for electrophoretic deposition. The maximum applied potential was -1.0 V *vs.* SCE in order to avoid Faradaic reactions, mainly the hydrogen evolution reaction that can form bubbles on the electrode surface, thus preventing deposition. A more dilute sol concentration of 3 g/l is used. Once the cell is complete, the potential is applied for a controlled period of time and removed to stop the coating process. In electrophoresis the sol concentration, applied voltage, and tool submersion time are the controlled variables. The tool withdrawal rate is not treated as a process variable for electrophoresis coating because it is not believed to play a significant role in determining the coating thickness due to the lower sol concentration. A table of the initial conditions chosen can be seen in Table 1.

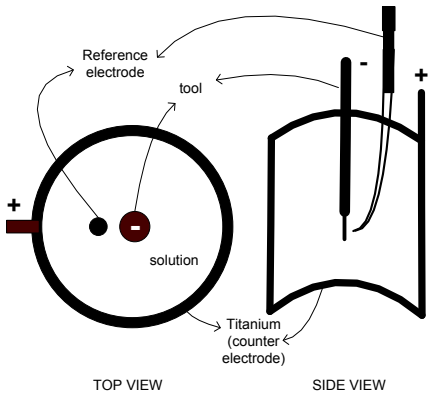

Fig. 1: Diagram of the electrodeposition setup.

The dip-coating and electrophoresis processes are currently both performed as batch processes with the same base sol formulation (different dilutions) and the micro end mills are treated identically before and after the coating process for both dip-coating and electrophoresis deposition. A generalized depiction of the coating process is given in Fig. 2. In this processing schematic, the "dip tools" step refers to the dip-coating and electrophoresis processes.

Table 1. Duration of electrophoretic deposition.

E / V vs. SCE	
-0.5 V	**-1.0 V**
5 min	5 min
-	7.5 min
10 min	10 min

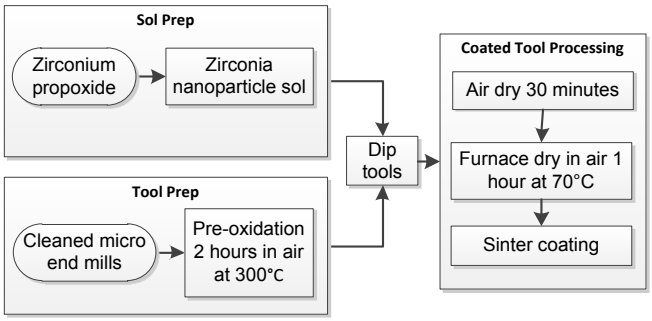

Fig. 2: Generalized process diagram of coating procedure.

EXPERIMENTAL PROCEDURE

Characterization of the coated tools was performed using scanning electron microscopy (SEM) and a white light optical metrology system (InfiniteFocus with Real3D by Alicona). The coating coherence was qualitatively judged by degree of coverage. The goal was to completely coat all surfaces of the tool, with emphasis in the cutting zone. The coating was detected by the change in surface morphology from the uncoated tools (SEM and optical) and the presence color fringes (optical). After coating, boundaries of WC grains on the tool surface were hidden, but striations from the tool manufacturing (grinding) process were still visible. When possible, the coating thickness was measured in areas of cracking to obtain a quantitative measurement of the coating thickness. Fig. 3 shows an SEM image from a partially coated tool illustrating the change in surface morphology caused by the coating. Special attention was also paid to the cutting edge during SEM characterization. The authors believe that insufficient coating at the cutting edge could provide an initiation site for cracking and delamination of the coating.

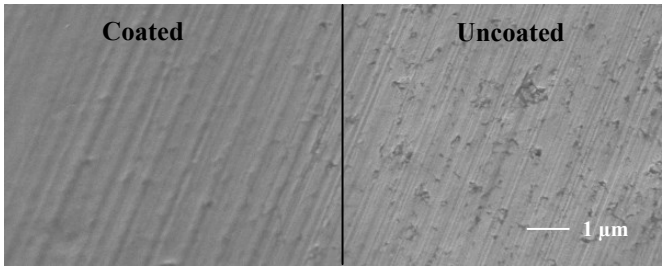

Fig. 3: SEM micrograph of micro end mill rake face surface showing the difference in surface morphology after coating.

Machining tests were performed using the coated tools to make full-width channels in 6061-T6 aluminum alloy using oil-based lubricant to evaluate coating performance over a 50 mm distance (6 sec machining time). Tests were performed on a CNC mill (HAAS TM-1) with a high-speed spindle (NSK HES510) mounted in the tool holder. The following machining parameters were held constant: 40,000 rpm spindle speed, 500 mm/min feedrate, 50 µm axial-depth-of-cut. Dynamic forces were recorded during machining using a 3-axis piezoelectric force dynamometer (Kistler model 9256C2) and the raw force data was post-processed to filter out signal noise and track machining forces associated with each cutting tooth along the length of the channel.

A destructive evaluation was also performed for an electrophoresis coated tool by casting the as-coated tool in epoxy-resin and creating a metallographic cross-section of the cutting zone by physically polishing in the axial direction from the tool tip. The cross-section view allows direct characterization of the coating-tool interface and morphology that may change along the thickness of the coating.

RESULTS

A. DIP-COATING

Initial SEM and optical characterization of tools coated with nanocrystalline zirconia using the sol-gel dip-coating method showed that coherent coatings with minimal cracking are possible, as seen in Fig. 4. The coating showed no cracking or agglomeration during the coating process. The light colored band observed near the tool tip in (b) is a result of charge accumulation during SEM imaging, indicating an area of greater coating thickness that is more resistant to electron flow due to the poor electrical conductivity of pure zirconia. This coating thickness variation was also observed in optical images where color fringes were seen (Fig. 5).

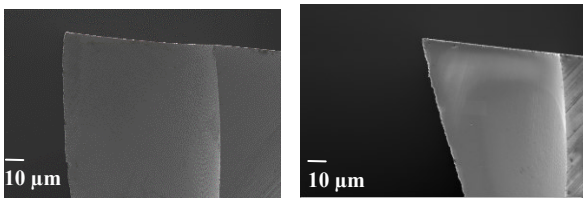

(a) (b)

Fig. 4: SEM micrographs of micro end mill in (a) uncoated and (b) ultra-thin nanocrystalline zirconia coated conditions.

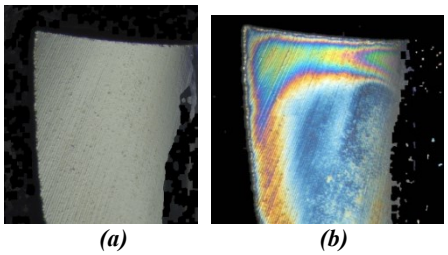

(a) (b)

Fig. 5: Optical images of an (a) uncoated micro end mill and (b) the same tool coated with ultra-thin nanocrystalline zirconia.

The color variation in the optical images is also of interest as a method of determining variations in coating thickness. This color variation is believed to be due to thin-film interference similar to the colors in a soap bubble. These images could potentially be used to quantitatively determine the

variation in coating thickness based solely on optical measurement. More work would be necessary to directly measure the coating thickness in cross-section for the various color regions to better define the relationship between observed color and coating thickness. Some work has already been done in relating observed color variations on a titanium substrate after controlled oxidation to the oxide scale thickness [5].

The coating thickness was found to depend greatly on the concentration of zirconia nanoparticles in the sol. Tools coated with a more concentrated sol (22 g/L) were found to exhibit more cracking in the region near the tip of the tool and occasionally showed coatings over 1 µm thick. Therefore, the less concentrated 11 g/l sol was subsequently used for all dip-coating trials.

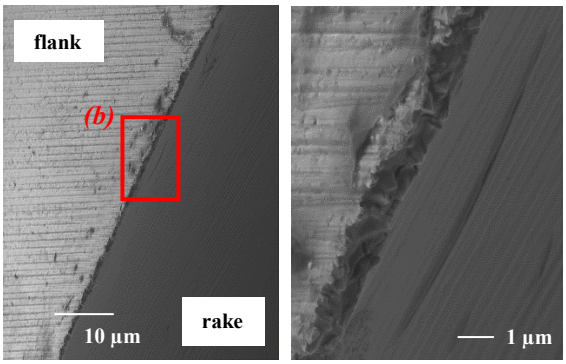

(a) *(b)*

Fig. 6: SEM images at the cutting edge of a micro end mill after dip-coating. Conformal coating is present on the rake face and at the edge. Little coating is present on the flank face.

The coating has been shown to be crack-free on the rake face of the tool in the region of chip flow using SEM (Fig. 4) and optical characterization (Fig. 5). However, it is also necessary that the coating be continuous around the cutting edge, or cracks could initiate at the coating-tool interface and delamination of the otherwise continuous coating would occur. SEM characterization was used to evaluate the coating at the cutting edge under high magnification to determine if the coating completely coated the cutting edge. Fig 6 shows the cutting edge of a micro end mill after dip-coating. Coating can be positively identified at the cutting edge by the presence of small cracks or separations in the areas between grains. However, it appears that the coating may be resting in between grains and not providing total coverage, providing potential crack initiation sites.

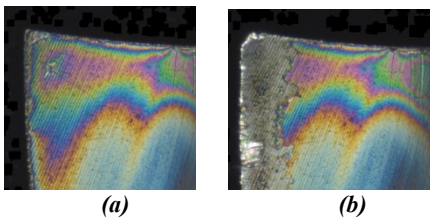

(a) *(b)*

Fig. 7: Optical images of a zirconia coated micro end mill before (a) and after (b) machining showing the area of removed coating.

Results from the initial machining tests with lubrication showed that the coating was consistently removed during machining on the rake face in the region of chip flow (Fig. 7). Forces were measured along the length of cut, but no significant or repeatable difference between the coated and uncoated micro end mills in terms of machining forces was found.

B. ELECTROPHORESIS

Initially, the electrophoresis process was performed using a deposition potential of -0.5 and -1.0 V at 3 g/l sol concentration. No significant change in the surface morphology was seen after 30 minutes at -0.5 V. The procedure was repeated at -1.0 V for 5, 7.5, and 10 minutes. The resulting coatings for these conditions are shown in Fig. 8. The coating resulting from 5 min of electrophoresis was determined to have poor coverage. The coating from a 10 minute deposition showed extensive cracking, presumably caused by a coating that was more than 200-nm-thick. The optimum condition for coating was determined to be near the 7.5 minute condition, where extensive coating was achieved without significant cracking. The coating thickness after 7.5 min was approximately 200 nm. Further investigation is necessary in order to optimize the electric field strength and deposition time.

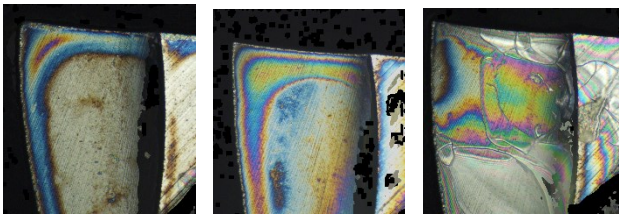

Fig. 8: Optical images of electrophoresis coated micro end mills after 5 min (a), 7.5 min (b), and 10 min (c).

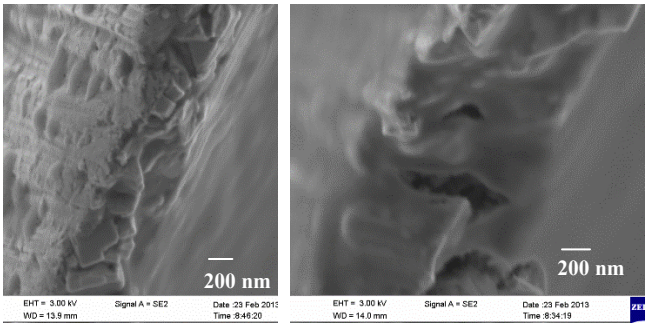

(a) *(b)*

Fig. 9: SEM images at the cutting edge after electrophoresis coating

Two tools were initially coated at -1.0 V for 7.5 min. Both tools were characterized with SEM after fully drying in the as-coated condition without sintering. The cutting edge was carefully characterized with SEM to evaluate the level of coverage. Fig. 9 shows an example of the typical morphology seen on the coated cutting edge after electrophoresis deposition. There are clear signs that coating is present, but the individual WC grains are still very distinct in Fig. 9(a). Other areas show very good coverage and the grain structure is almost completely masked Fig 9(b). It is important to note that these images came from the same cutting tool and show that variation may occur along the length of the cutting edge. The reasons for this variation are still unclear. In areas where the coating is thicker on the cutting edge, the coverage looks

very good, but cracks and separations in the coating are also evident and may act as delamination initiation sites during the actual machining process.

One tool was then immediately cast into epoxy and polished to obtain a metallographic cross-section to examine the coating-tool interface in the unsintered condition (Fig. 10). The second tool was sintered, sonicated in methanol, characterized with SEM, used to machine 6061-T6, and characterized again with SEM (Fig 11). The goal of the destructive metallographic evaluation was to obtain a cross-section of the undisturbed coating interface. This would allow a direct and accurate evaluation of the coating thickness distribution and hopefully relate this to the colors seen in the optical metrology to obtain another measurement technique for determining the thickness. The cross-section would also allow measurement of coating porosity and hardness. It should be noted that due to the small size of the coating particles (~3 nm) it has not yet been possible to quantify the porosity. IN future work, atomic force microscopy (AFM) is proposed to measure the coating properties in cross section because of the potential for atomic level resolution. Also, the AFM can be used as a nano-indenter to gauge the hardness of the coating locally.

An epoxy was chosen because of the ability to cast at room temperature so as not to affect the coating structure. However, during the polishing process, there was an unexpected twisting of the tool in the epoxy mount. Fig. 10(a) shows the cavity left behind due to this twist. This disturbance caused a separation of the coating from the tool and made accurate thickness measurements impossible. An interesting result from this separation is that the majority of the zirconia coating remained adhered to the epoxy while a thin layer of coating remained on the tool surface, indicating that the failure occurred internally rather than at the tool interface as seen in Fig 10(c) and (d). This could be evidence of a successful interfacial bond, but further trials are necessary to obtain a cross-section with an undisturbed tool-coating interface.

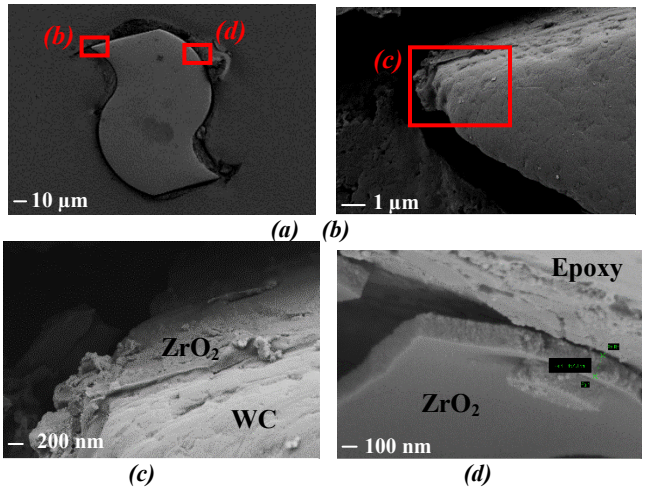

Fig. 10: SEM images of an unsintered zirconia coated micro end mill cast in epoxy and polished in the axial direction. Overall view (a), cutting edge (b) and high magnification (c, d).

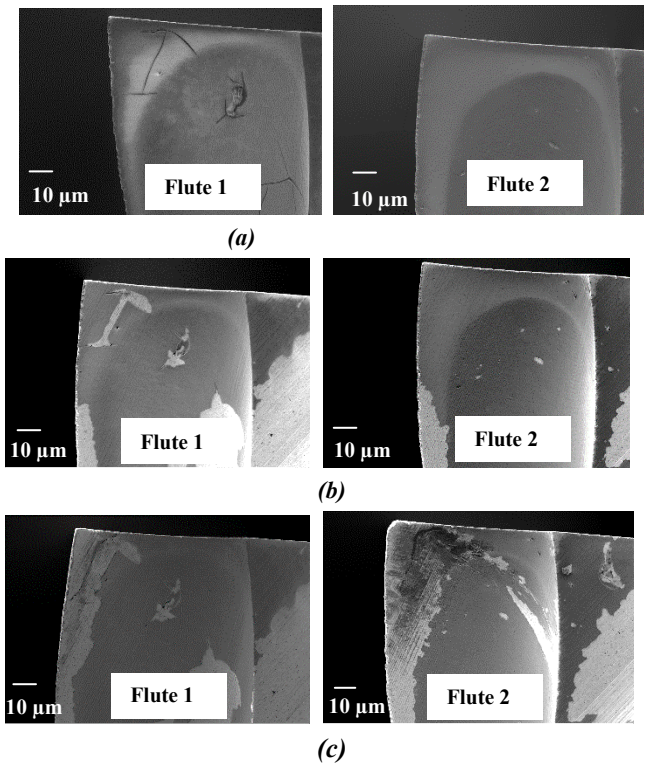

Fig. 11: Optical images of a zirconia coated micro end mill (a) before machining and (b) after machining for 50 mm.

The second tool was evaluated in machining to evaluate the coating behavior under actual processing conditions. After sintering for 1 hour at 850°C, the tool was held with the cutting tip submerged into a methanol bath and placed into an ultrasonicator for 15 minutes. The result is shown in Fig. 10 (b). Fig. 10 (b) shows that areas of pre-existing cracking are likely to be removed during ultrasonication. Some other areas that did not show prior cracking were also removed. These areas appear to coincide with surface agglomerations or areas of thicker coating that might be more affected by the tool vibration. This method provided a quick and easy step for evaluating the potential for coating delamination during subsequent machining.

The tool was then used to machine 6061-T6 aluminum alloy with oil-based cutting fluid for 6 seconds at a chipload of 6.25 µm (50 mm distance at 500 mm/min and 40,000 rpm). Two uncoated new micro end mills were also used to machine under these conditions to provide a baseline for the tool condition after machining. The result observed in Fig. 10 (c) for the coated micro end mill was the absence of coating in the cutting region after machining. This result indicates that the coating was physically removed very quickly during machining. It is not yet clear what the exact removal mechanism was (abrasion or flaking). The coating was shown to be largely undisturbed in areas outside the region of chip flow, but completely removed within the region of chip flow.

A comparison of the coated and uncoated micro end mills after machining can be seen in Fig 12. The direction of chip flow can be seen clearly for the coated tool in (b) and is indicated by the directionality of the shallow grooves and smears of aluminum and zirconia in the vicinity of the cutting

edge.

Fig. 12 shows evidence of gradual abrasive wear on the tungsten carbide tool surface after the oxide coating has delaminated. This means that the coating delaminated very early in the 6 second machining test and that the tool substrate has not been significantly weakened by the sol-gel process.

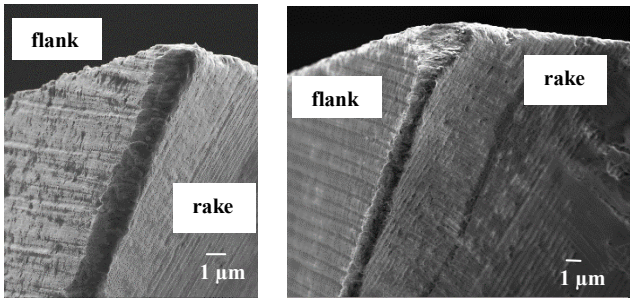

(a) *(b)*

Fig. 12: Optical images of a zirconia coated micro end mill (a) before machining and (b) after machining for 50 mm.

CONCLUSIONS

Micro end mills are extremely fragile compared to the larger mills used in conventional machining and this limits the feed and thus material removal rate. Methods of enabling more aggressive machining should be found to improve micro end milling productivity without adding a large cost per tool. Sol-gel deposition methods have been shown to create thin conformal oxide coatings with good coverage and are economically feasible.

By choosing the correct control parameters both with respect to dipping and electrophoretic deposition one can deposit a submicron crack-free layer of sol-gel derived zirconia oxides on the surface of micro-cutting tools. From images derived from both SEM and visible light microscopy, one could see that thicker films were produced near the edges of the tools using dip-coating, rather than by electrophoretic deposition. We believe that this may be due to the surface tension of the suspension that does not allow the suspension to flow uniformly on surfaces that are not flat. Therefore, electrophoretic deposition, particularly with respect to edges, may allow one to produce more uniform films.

It was found that by dipping a coated and sintered tool into an ultrasonic bath one can dislodge areas of coating that are not firmly attached to the surface. This is an easy way of quickly testing adhesion without performing any actual machining. While tests with respect to machining for both dip-coated and electrophoretically deposited coatings have not yet provided positive results this fact does not allow us to distinguish between adhesion of the film to the surface of the tool or to hardness of the film during milling. Further work is necessary to address these durability issues so as to decide whether hardness or adhesion or both are related to the efficacy of these coatings in actual practice.

Lastly, it is also important to note that in no way has the coating process negatively affected the tool substrate through chemical interactions or increased temperature. We suggest that this is not necessarily true for all coating techniques.

FUTURE WORK

Ongoing work will focus on investigating the root cause of the coating delamination during machining. The coatings currently obtained through dip-coating and electrophoresis deposition of pure zirconia on tungsten carbide micro end mills do not survive the machining process. The reasons for this are still unclear, but may be tied to achieving proper coating densification and adhesion during sintering. This will lead to additional work evaluating the pretreatment and coating sintering processes to improve the coating adhesion and durability.

Coating adhesion will be qualitatively evaluated with ultrasonication to expedite the development process. Once a coating consistently survives the ultrasonication process end milling tests will be used to further characterize the adhesion. Once a more durable coating is obtained, the machining forces will be collected and compared between coated and uncoated tools under similar conditions. Other important comparisons to be drawn from the machining work is the relative wear of the coated and uncoated tools and any differences in tool life.

Further study is also needed to improve the destructive metallographic evaluation method. This method is promising because of the potential for obtaining direct thickness measurements, coating porosity, and hardness. The first attempt showed that while the epoxy mounting media did form a good bond with the coated tool, the epoxy was not stiff enough to prevent tool movement during the polishing process. Therefore changes may be needed to the polishing process or to the mounting material to prevent twisting or other movement to obtain an undisturbed tool-coating interface cross-section. This evaluation method also ties in directly with relating the colors observed with optical microscopy of the coating to the actual coating thickness. Future work will hopefully find a definitive relationship between the color and the thickness. Tools could then be developed for relating the color value at every visible point on the tool surface to a coating thickness and plotting the spatial coating thickness distribution. It remains to be seen if any corrections for the helical flute geometry will need to be made for accurate results.

Both the dip-coating and electrophoresis processes could potentially be extended to other oxide systems including aluminum oxide and partially stabilized zirconia (PSZ). The behavior of these coatings on micro end mills during machining should also be evaluated and compared to the pure zirconia coatings presented here.

ACKNOWLEDGMENTS

The authors would like to gratefully acknowledge the University of Wisconsin-Madison for support through the Innovation and Economic Development Research (I&EDR) grant and thank Dave Burton from Performance Micro Tool, Inc. for supplying tools.

REFERENCES

[1] C. D. Torres et al., "Analyzing the performance of diamond-coated micro end mills," *Int. J. Mach. Tool Mfg.*, 2009; vol. 49: pp. 599–612.

[2] A. Aramcharoen et al., "Evaluation and selection of hard coatings for micro milling of hardened tool steel," *Int. J. Mach. Tool Mfg.*, 2008; vol. 48: pp. 1578–1584.
[3] W. D. Sproul, "Physical vapor deposition tool coatings," *Surf. Ctg. Tech.*, 1996; vol. 81: pp. 1–7.
[4] Y.-C. Chen, X et al., "Preparation of α-alumina coated carbide tools by the sol-gel process," *Mtl. Sci. Eng., 2000;* vol. 288: pp. 19–25.
[5] "Thermal Spray Technologies," Available online: http://www.tstcoatings.com/
[6] R. Caruso et al., "Controlled preparation and characterization of multi-layer sol-gel zirconia dip-coatings," *J. Mater. Res.,* 2001; Vol. 16, No. 8. pp. 2391-2398.
[7] C.J. Brinker et al., "Review of sol-gel thin film formation," *J. of Non-Crystalline Solids*, 1992; vol. 147&148, pp. 424-436.
[8] A. Pfrengle et al., "Electrophoretic deposition and sintering of zirconia layers on microstructured steel substrates," *J. of the Eur. Cer. Soc.*, 2006; vol. 26, pp. 2633–2638.
[9] D.R. Uhlmann and G. Teowee, "Sol-Gel Science and Technology: Current State and Future Prospects," *J. Sol-Gel Sci. and Tech*, 1998; vol. 13, pp153-162.
[10] Q. Xu and M. Anderson, "Sol–Gel Route to Synthesis of Microporous Ceramic Membranes: Preparation and Characterization of Microporous TiO2 and ZrO2 Xerogels," *J. Amer. Cer. Soc.,* 1994; vol. 77, no. 7, pp. 1939-1945.
[11] M. V. Diamanti et al., "Interference colors of thin oxide layers on titanium," *Color. Res. & App.*,2008; vol. 33: pp. 221–228.